Chapter 2

Physical Fundamentals and Employed Methods

In this chapter, a brief summary of the physical fundamentals and optimization strategies will be given. The molecular systems will be discussed when first encountered in an experiment.

2.1 A Brief Introduction to Molecular Dynamics

The time-dependent Schrödinger equation

$$i\hbar\frac{\partial\psi(\mathbf{x},t)}{\partial t} = H_0\psi(\mathbf{x},t) \tag{2.1}$$

can be used to describe the dynamics of an isolated molecule. With no external field applied, the Hamilton operator H_0 and the molecular potentials are time-independent. The solution of the time-dependent Schrödinger Equation (TDSE) can be written as [29]

$$\psi(\mathbf{x},t) = \sum_{n=1}^{\infty} a_n\psi_n(\mathbf{x})e^{-\frac{i}{\hbar}E_nt} \tag{2.2}$$

describing a wavepacket[1] whose expectation values change in time. When calculating the probability density $|\psi(\mathbf{x},t)|^2$

$$|\psi(\mathbf{x},t)|^2 = \sum_{m,n=1}^{\infty} a_m^*a_n^*\psi_m^*(\mathbf{x})\psi_n(\mathbf{x})e^{-\frac{i}{\hbar}(E_n-E_m)t} \tag{2.3}$$

it is apparent that at least two different energetic levels (eigenstates) E_n and E_m have to exist for the wavepacket to evolve. For a coherent state, the expectation value of $<\hat{x}>_t$ is

$$<\hat{x}>_t = \int \psi^*(\mathbf{x},t)\hat{x}\psi(\mathbf{x},t)d\mathbf{x} \tag{2.4}$$

[1] if Gaussian, it is also considered to bear minimum uncertainty as its form satisfies the uncertainty relation $\Delta x \cdot \Delta t = \hbar/2$

which can be considered as the movement of a classical particle, in accordance with the Ehrenfest theorem.

Irradiating a molecule with a coherent (linearly polarized) laser field leads to a time-dependent Hamiltonian, which consists of

$$H_0 = -\frac{\hbar^2}{2m}\nabla^2 + V_M(\mathbf{x}) \tag{2.5}$$

and a time dependent part as

$$H = H_0 + H_1. \tag{2.6}$$

with $V_M(\mathbf{x})$ as the molecular potential and H_1 as the disturbance caused by the laser field. For weak laser fields, this can be stated using the dipole approximation as $H_1 = -\mathbf{E}(t) \cdot \boldsymbol{\mu}$ where the significance of the vectorial nature of light can already be anticipated which will be exploited for the polarization experiments described in this thesis.

Using the Born-Oppenheimer approximation, the TDSE can be written as

$$i\hbar\frac{\partial}{\partial t}\begin{pmatrix}\psi_a(t)\\ \psi_b(t)\end{pmatrix} = \begin{pmatrix} H_a & -\boldsymbol{\mu}_{ab}\cdot\mathbf{E}^*(t) \\ -\boldsymbol{\mu}_{ba}\cdot\mathbf{E}(t) & H_b\end{pmatrix}\begin{pmatrix}\psi_a(t)\\ \psi_b(t)\end{pmatrix} \tag{2.7}$$

where $\psi_a(t)$ and $\psi_b(t)$ are the wave functions of the two employed electronic transitions, with H_a and H_b as their respective Hamiltonians, which determine the dynamics of the electronical states. First order perturbation theory yields for small disturbances:

$$\psi^{(1)}(\mathbf{x},t) = \frac{1}{i\hbar}\int_0^t e^{-\frac{i}{\hbar}H_b^{(0)}(t-t')}\big[-\boldsymbol{\mu}_{ba}\cdot\mathbf{E}(t')\big]e^{\frac{i}{\hbar}H_a^{(0)}(t')}\psi_a(\mathbf{x},0)dt'. \tag{2.8}$$

A system which resides in the lowest vibrational state of the electronical ground state at $t = 0$ propagates according to $H_a^{(0)}$. An interaction of the light field at t' with the molecule's dipole moment transfers the population to an excited state, spread over many neighbouring vibrational states due to the spectral width of the pulse. The created wavepacket therefore consists of a superposition of states and evolves according to $H_b^{(0)}$ and the corresponding phase factors. Eq. 2.8 can also be expressed in a basis of the vibrational eigenfunctions of the electronically excite state $\psi_{v',b}(\mathbf{x})$ as

$$\psi^{(1)}(\mathbf{x},t) = \sum_{v'} e^{-\frac{i}{\hbar}E_{b,v'}t}\psi_{b,v'}(\mathbf{x})\cdot c_{v',v''}\cdot I_{v',v''}(\omega,t) \tag{2.9}$$

with the time-dependent part

$$I_{v',v''}(\omega,t) = \int_0^\infty F(t')e^{\frac{i}{\hbar}(E_{b,v'}-E_{a,v''}-\hbar\omega)t'}dt' \tag{2.10}$$

where $F(t')$ is a time dependent amplitude, and a factor which is a product of transition dipole moment and Franck-Condon integral

$$c_{v',v''} = \int \psi_b(\mathbf{x}')\boldsymbol{\mu}_{ab}^{el}\psi_a(\mathbf{x}')d\mathbf{x}' \cdot \int \psi_{v'}(\mathbf{x})'\psi_{v''}(\mathbf{x})d\mathbf{x}. \tag{2.11}$$

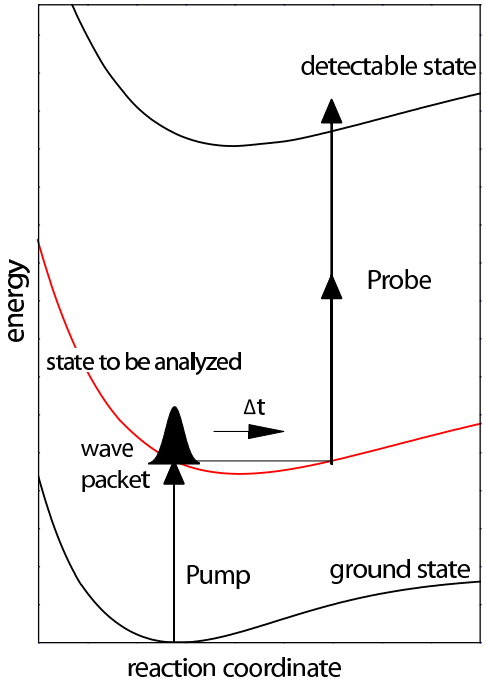

Figure 2.1: Schematic illustration of a pump-probe experiment, where a pump-pulse prepares a wavepacket in the state that is to be analyzed. A probe pulse after a time duration Δt transfers the created population to the detectable state.

The interaction time from one vibronic to another vibronic state is short ($< 10^{-15}$ s) compared to typical vibrational frequencies, and it can be assumed to occur at a constant nuclear distance. Transitions are also more likely to occur at turning points where there is a greater overlap of the respective wave functions. The coherence of the exciting pulse is transferred to the excited state where it imposes its phase factor to individual vibrational states, which then evolve in time. Shaped laser pulses (with complicated phase and amplitude factors) can therefore be employed to selectively induce interference effects in the wavepacket's propagation.

The pump-probe technique [30, 31] (see Fig. 2.1) is a common tool to study wavepacket propagation on such electronically excited states, whereby two ultrashort pulses sequentially irradiate a molecular sample. The first sub pulse excites the molecule from a ground to an excited state, and the second pulse transfers to a final state (which is an ionic state in this work). The time difference $\Delta t = t'' - t'$ can be found in the solution of the time dependent Schrödinger equation using second order perturbation theory [32]

$$\psi^{(2)}(\mathbf{x},t) = \left(\tfrac{1}{i\hbar}\right)^2 \int_0^t \int_0^{t'} e^{-\frac{i}{\hbar}H_c(t-t')}\big[-\boldsymbol{\mu}_{cb}\cdot\mathbf{E}(t')\big]e^{-\frac{i}{\hbar}H_b(t-t'')}\big[-\boldsymbol{\mu}_{ba}\cdot\mathbf{E}(t'')\big]\cdot e^{-\frac{i}{\hbar}H_a t''}\psi_a(\mathbf{x},0)dt'dt''. \tag{2.12}$$

With resonant intermediate states, multi-photon processes may also be incorporated, this method is called REMPI (resonance enhanced multi-photon ionization process) with either neutral [33] or ionic [34] target states.

2.2 Mathematical description of fs-laser pulses

The electrical field of a fs-laser pulse $E(t)$ in the time-domain consists of superposed, complex frequency components

$$E(t) = \frac{1}{2\pi} \int_{-\infty}^{+\infty} d\omega \ \tilde{E}(\omega) e^{i\omega t} \tag{2.13}$$

since $E(t)$ is a physical quantity and therefore real. The complex spectral field can be calculated by inverse Fourier transformation

$$\tilde{E}(\omega) = \int_{-\infty}^{+\infty} dt \ E(t) e^{-i\omega t}. \tag{2.14}$$

Excluding the negative frequencies by integrating from 0 to $+\infty$, is called $\tilde{E}^+(t)$, whereby the remaining integral is sometimes called $\tilde{E}^-(t)$. Using $\tilde{E}^+(t)$ and $\tilde{E}^+(\omega)$ ensures that there are only positive frequency components, since $\tilde{E}^-(\omega)$ is by definition zero[2] for all $\omega \geq 0$. In the following, the $^+$ and $\tilde{}$ will be disregarded for simplicity. For pulse lengths that comprise of several optical cycles (where the slowly varying envelope approximation can be applied) an envelope, or amplitude $F(t)$

$$E(t) = F(t) \cdot e^{i\Gamma(t)} \tag{2.15}$$

can be assigned. The change in $\Gamma(t)$ defines an instantaneous frequency

$$\frac{d\Gamma(t)}{dt} = \omega_0 + \frac{d\varphi(t)}{dt}. \tag{2.16}$$

Also, $\Gamma(t)$ can be separated in a fast and a slow oscillating term leading to

$$E(t) = \underbrace{e^{i\omega_0 t}}_{fast\ term} \cdot \underbrace{F(t)}_{temp.ampl.} \cdot \underbrace{e^{i\varphi(t)}}_{temp.phase} \tag{2.17}$$

Polynomial temporal phase. $\varphi(t)$ can be expanded in a Taylor series as

$$\varphi(t) = a_0 + a_1(t-t_0) + \frac{1}{2}a_2(t-t_0)^2 + \frac{1}{6}a_3(t-t_0)^3 + \frac{1}{24}a_4(t-t_0)^4 + \dots \tag{2.18}$$

with the coefficients

$$a_n = \frac{d^n}{dt^n}\varphi(t)|_{t=t_0}, \tag{2.19}$$

whereby a_0 is the relative position of the rapid oscillations with respect to the envelope, a_1 is the central frequency shift, a_2 the so-called linear chirp, which corresponds to a linear change of the instantaneous frequency in time, etc.

[2] whereby $\tilde{E}^+(t) + \tilde{E}^-(t) = E(t)$ still reassembles the original real field

Polynomial spectral phase. Similarly, $E(\omega)$ can be written as

$$E(\omega) = G(\omega)e^{i\varphi(\omega)}. \tag{2.20}$$

A linear filter such as an ideal pulse shaper can be stated as complex filter function

$$\tilde{H}(\omega) = R(\omega) \cdot e^{i\phi(\omega)} = \sqrt{T(\omega)}e^{i\phi(\omega)} \tag{2.21}$$

with $R(\omega)$ as amplitude modulation, which is the square root of the transmission $T(\omega)$. An input pulse $E_{in}(\omega)$ that is modulated by the filter $\tilde{H}(\omega)$ has the form

$$\tilde{E}_{out}(\omega) = \tilde{H}(\omega) \cdot \tilde{E}_{in}(\omega). \tag{2.22}$$

The spectral intensities can be derived directly from the transmission $T(\omega)$ when multiplying with the input pulse's envelope

$$I(\omega) \propto \left|\tilde{H}(\omega) \cdot E_{in}(\omega)\right|^2 = |E_{in}(\omega)|^2 \cdot T(\omega). \tag{2.23}$$

The phase "filter" $\phi(\omega)$ can be expanded in a Taylor series as

$$\phi(\omega) = b_0 + b_1(\omega - \omega_0) + \frac{1}{2}b_2(\omega - \omega_0)^2 + \frac{1}{6}b_3(\omega - \omega_0)^3 + \dots \tag{2.24}$$

with the expansion coefficients

$$b_n = \frac{d^n}{d\omega^n}\phi(\omega)|_{\omega=\omega_0}. \tag{2.25}$$

The effects of the coefficients on a pulse in the time domain vary; for example b_0 shifts the field beneath the envelope; b_1 corresponds to an envelope shift in time, b_2 is the linear chirp of the pulse which causes a linear increase or decrease of the instantaneous frequency, b_2 is the quadratic chirp which causes an asymmetric pulse trail, and b_3, the third order chirp, leads to a symmetric offset of the pulse's baseline; more examples can be found in Refs. [35, 36].

2.3 Birefringence and Liquid Crystal Modulators

In isotropic and linear media like glasses, light propagates the same for all directions, yielding the relation between the displacement field $\mathbf{D}$ and the electric field $\mathbf{E}$

$$\begin{aligned} \mathbf{D} &= \varepsilon_0\mathbf{E} + \mathbf{P} \\ \mathbf{P} &= \chi\varepsilon_0\mathbf{E}, \end{aligned} \tag{2.26}$$

where ε_0 is the permittivity of free space and $\mathbf{P}$ the vector field that is related to the electric dipole moments present in the medium. This leads to $\mathbf{D} = \varepsilon\mathbf{E}$ with $\varepsilon = \varepsilon_0(1 + \chi)$. For anisotropic media that have preferential directions such as crystals, $\mathbf{P}$ is not inevitably aligned along $\mathbf{E}$. The former relationships have to be expressed by $\mathbf{P} = \varepsilon_0\boldsymbol{\chi} \cdot \mathbf{E}$, where $\boldsymbol{\chi}$ is called the electric susceptibility tensor. It can be concluded that $\mathbf{D}$ and $\mathbf{E}$ are also related tensorically as

$$\mathbf{D} = \varepsilon_0\mathbf{E} + \mathbf{P} = \varepsilon_0\mathbf{E} + \varepsilon_0\boldsymbol{\chi} \cdot \mathbf{E} = \varepsilon_0(1 + \boldsymbol{\chi}) \times \mathbf{E} = \varepsilon_0\boldsymbol{\varepsilon} \cdot \mathbf{E}. \tag{2.27}$$

whereby $\boldsymbol{\varepsilon}$ is called the dielectric tensor, which means that also the refractive index of the medium must be a tensor, leading to the phenomenon called birefringence. A liquid crystal modulator uses nematic crystals which are elongated molecules that have a preferred spatial orientation, but are not fixed in space (unlike a crystal), meaning that the liquid has an anisotropic dielectic tensor. Rotation of the molecules, induced by an electric field (which is created by applying a voltage V) therefore goes along with a change of the index of refraction. A liquid crystal cell acts upon an incoming light field as a birefringent crystal with a fast and a slow axis. The glass plates are brushed to provide an initial alignment of the molecules[3], with different indices of refraction along these axes. The phase retardance[4] between the extraordinary and the ordinary index beam of a liquid crystal with thickness d at a wavelength λ_0 is

$$\Gamma = \frac{2\pi d}{\lambda_0}(n(\theta) - n_0) = \frac{2\pi d}{\lambda_0} n(V), \tag{2.28}$$

whereby $n(V)$ is the voltage dependent index of refraction that is obtained by calibration [37, 36, 38].

2.4 Evolutionary Algorithms

Evolutionary algorithms (EAs) are used for combinatorial optimization [39] and are appointed to problems which are expected to be hard to solve, and when no other methods have proved efficient or successful.

The optimization technique employed throughout this work is the so-called evolution strategy which originates from the German word "Evolutionsstrategie". It is based on concepts from biological evolution, mutation, recombination, and survival-of-the-fittest [11]. To solve a problem, evolution strategy, usually applied for problems with smooth fitness landscapes, uses a set of individuals which together constitute a population. Each individual has a genome, which is represented by the real-valued objective variables $\vec{x}$. The individuals undergo change like mutation and recombination to adapt to their "environment" which is quantified by a "fitness" function. The fittest individuals survive, until, if successful, an optimal solution is found after a certain number of iterations. Like in biology, there is a distinction between the genetic encoding (genotype) and the actual physiological manifestation (phenotype).

Evolution strategy is only a sub-class of the more general, evolutionary algorithms which differ in the preferred way of implementing the above mentioned types of natural principles [40]. Genetic algorithms (GAs) [12, 41, 42] are popular for binary-coded problems, evolutionary programming (EP) [43] allows the numerical parameters of the program to evolve, and genetic programming (GP) [44] has subprograms which compete for the best ability to solve a problem.

All these variants are embedded in the more general scheme of so-called metaheuristic algorithms [45]. A heuristic[5] algorithm is more or less an educated guess

[3] which was $\pm 45°$ for this work

[4] in the linear regime, where intensity changes do not influence the phase modulation

[5] Ancient Greek "heurisko" means "I find"

that directs the search for solutions in areas that are poorly understood. Meta-heuristic strategies provide "meta" methods to direct heuristic algorithms toward the optima, and are very generally applicable, but not always efficient. They include local search [46], simulated annealing [47], Tabu search [48, 49], Ant Colony Optimization [50], the Greedy Randomized Adaptive Search Procedures (GRASP) [51], but also cover topics such as self-organization, artificial life, and swarm intelligence. The central focus of meta-heuristics is finding the right balance between "diversification" which enforces novelty and "intensification", which enforces quality. In a biological analogy, the problem of exploiting a niche for "resources", which is a short-term optimization goal, can very often conflict with the more long-term goal of exploration of other, more distant and possibly more fertile niches. If too much exploring is carried out, the algorithm starts to resemble a random search with no convergence; if too much exploitation of niches is performed, a convergence to local optima is likely to be the case.

Employed algorithm. There are two types of gene-encodings for this thesis, the so-called "free optimization" will be presented here, as it is a prerequisite for Chapters 4 and 5. "Parametric optimization" will be explained in detail in Chapter 6. Free optimization makes use of every possible parameter, which in the case of a liquid crystal modulator are all its N single pixels, and an assignment pixel $\leftrightarrow$ gene seems to be very straightforward. For phase shaping the objective variables are defined as $\vec{x} = \{\phi_1, \cdots, \phi_N\}$; adding the amplitude can be stated as $\vec{x} = \{T_1, \cdots, T_N, \phi_1, \cdots, \phi_N\}$ whereby the transmissions T_i and phase filter values ϕ_i are set by the respective shaper pixels.

If not stated otherwise, the algorithm (Fig. 2.2) and the following settings have been used throughout this work:

The algorithm starts with a population of the size λ with a random distribution of the gene values within the encoding boundaries (*initialization*), which leads to expectation values of $\bar{\phi} = 0$ and $\bar{T} = 0.5$ due to their encoding range T: $[0, 1]$ and ϕ: $[-\pi, \pi]$. The population is then probed (*evaluation*), for example by measuring a molecular ion signal, and one[6] fitness value $f(\vec{x})$ is assigned per individual.

The individuals, at this point called parents, will procreate; deterministic *selection* permits the μ parents with the highest fitness values to do so. Another variant, tournament selection, would select parents probabilistically, where each parent has a chance that is directly proportional (or modified with some cost function) to its fitness.

The selected parents are then *recombined* to produce a λ-sized offspring (by choosing two random parents λ times) by uniform crossover. There, the genes of the two parents are randomly shuffled (without changing index) with a chance of fifty percent to originate from either parent A or B; similarly to the sketch below (using G, R, and B as possible values).

$$\left.\begin{array}{l}(GRBGBRBGGBGBG)\\(RRBRGBRGRBBGB)\end{array}\right\} \rightarrow \ (GRBRGBRGRBGGB)$$

Other characteristics of the new offspring individual, like fitness, will be randomly

[6] or more fitnesses, if multiplhavinge goals are to be optimized (see Chapters 4 and 9)

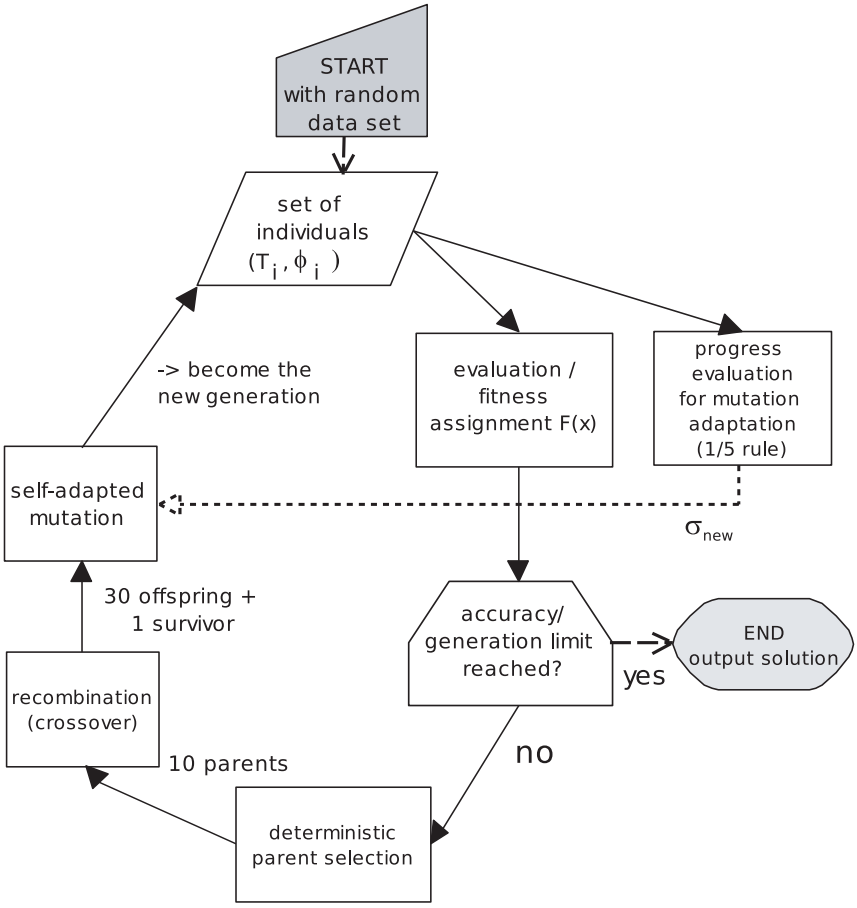

Figure 2.2: Sketch of the employed evolution strategy.

inherited from one of its parents. Compared to other methods of recombination like two-point crossover where two cut points in the chromosome are selected, and intermediate crossover, where the specific genetic values of the parents are averaged, uniform crossover produces a massive amount of randomness, but outperforms the others in many cases [52].

For the next iteration, all parents are discarded, except for the best individual. This improves the performance under noisy conditions, as noise may kill off the best individuals and advance inferior solutions, which, to a degree, introduces "elitism". For an environment without noise (like test problems), elitism may cause the population to become stuck in local optima because an once-found solution will only be replaced if an individual with a higher fitness emerges. On the other hand, certain global optima are more easily found when elitism is involved, as certain "lucky guesses" will not be discarded so easily.

The final step is self-adapted *mutation*, which adds a random number from a Gaussian distribution $N_i(0, \sigma)$ with the width σ and the expectation value 0 to every gene as

$$x_i' = x_i + N_i(0, \sigma). \tag{2.29}$$

Mutation, in the presented algorithm, is not parameter specific, it affects the transmission at the same rate as the phases (except for a factor of 2π), which is called

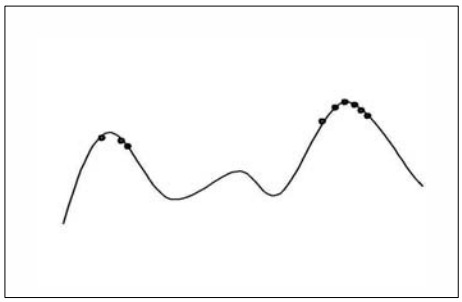

Figure 2.3: Capability of an evolutionary algorithm to climb two hills (explore two niches) at the same time, illustrated for a 1D fitness landscape, where each dot constitutes an individual.

single step size self-adaptation[7].

The self-adaptive mutation is implemented by evaluating the progress of the child population compared with the parent's. For the adaptation of the mutation width, Rechenberg's one-fifth rule [11] is applied, meaning that if more than 20% of the offspring perform better, the mutation stepwidth σ is counterintuitively (but ingeniously) increased by the factor of 1.25 for the next generation and otherwise decreased by the factor of 0.8.

The balance between exploration and exploitation is upheld by crossover on the one hand where unlike in nature, the mating pool is usually not limited to a specific niche, and a mutation operator, which is adapted according to the improvement of a current individual respective to its parent. After that, the mutated individuals are passed on to the next iteration, where they are evaluated, selected, etc., until the termination criterion is reached.

[7]The strategy to assign an individual mutation parameter σ_i or an rotation angle in a covariance matrix to every gene/pixel was not employed for this work as the used parameters are conceptionally similar.